

The Effect of Cr and Si Additions on the High-Temperature Atmospheric Corrosion of Fe–Ni Alloys: A Transmission Mössbauer Spectroscopy Study

R. IDCZAK^{a,b,*} AND R. KONIECZNY^a

^aInstitute of Experimental Physics, University of Wrocław, pl. M. Borna 9, 50-204 Wrocław, Poland

^bInstitute of Low Temperature and Structure Research, Polish Academy of Sciences,

Okólna 2, 50-422 Wrocław, Poland

(Received January 30, 2018; in final form September 7, 2018)

The high-temperature atmospheric corrosion of Fe–Ni, Fe–Ni–Cr and Fe–Ni–Si alloys was studied using the ⁵⁷Fe transmission Mössbauer spectroscopy. The transmission Mössbauer spectroscopy measurements were performed for samples after annealing process in vacuum as well as after the exposure to air at 870 K. The analysis of the obtained spectra gives an important information about changes of chemical composition and formation of iron oxides in studied samples during air exposure. The results reveal that the addition of a few atomic percent of Si has a significant effect on corrosion resistance of Fe–Ni alloys. In the case of Fe–Ni–Cr samples the effect is much less noticeable and the observed oxidation behaviour is quite similar to Fe–Ni and Fe–Cr alloys.

DOI: [10.12693/APhysPolA.134.1137](https://doi.org/10.12693/APhysPolA.134.1137)

PACS/topics: iron alloys, Mössbauer spectroscopy, high-temperature corrosion, atmospheric corrosion

1. Introduction

In our previous works, we have used ⁵⁷Fe Mössbauer spectroscopy for the investigation of high temperature atmospheric corrosion of α -Fe as well as diluted Fe–Cr and Fe–Si alloys [1–3]. As it was shown, this experimental technique gives a valuable information about changes of chemical composition and formation of iron compounds in studied material caused by corrosion process [4, 5].

In the present work, we decided to extend these investigations to Fe–Ni, Fe–Ni–Cr and Fe–Ni–Si alloys. These alloys as well as commercial steels based on them are used for a wide variety of applications due to their good soft magnetic properties as well as a low thermal expansion between room temperature and their Curie temperature caused by the Invar-effect [6–8]. Beside these physical properties also the corrosion behaviour under the environmental condition is important, because the physical properties can be influenced in a negative way by corrosion. Here, it is worth noting that the Mössbauer study of oxidation of Fe–Ni alloys in air at high temperature was presented by Channing et al. in their classical work [9]. They showed a systematic growth of various iron oxides in Fe–Ni alloys, with four different Ni content, during exposure to air at 535 and 635 °C. Moreover, their results indicate that with increase of Ni content of the alloy, the oxidation rate decreased. At the same time, in available literature, there is a lack of complex Mössbauer corrosion studies of

ternary Fe–Ni–Cr and Fe–Ni–Si alloys. Taking these facts into account, in present work, the emphasis was placed on determination of changes of Fe–Ni corrosion behaviour caused by addition of small amounts of Si or Cr.

2. Experimental details

2.1. Samples preparation and measurements

The samples of Fe_{0.97}Ni_{0.03}, Fe_{0.95}Ni_{0.05}, Fe_{0.94}Ni_{0.03}Cr_{0.03}, Fe_{0.92}Ni_{0.03}Cr_{0.05}, Fe_{0.94}Ni_{0.03}Si_{0.03}, and Fe_{0.92}Ni_{0.03}Si_{0.05} alloys were prepared in an arc-melting furnace under argon atmosphere. Appropriate amounts of the 99.995% pure chromium, 99.99% pure nickel, 99.95% pure silicon, and 99.98% pure iron were placed into a water-cooled copper crucible and melted twice to ensure homogeneity. The weight losses caused by a melting process was below 0.15% of the initial weight so it was assumed that the chemical compositions of the obtained ingots were close to nominal ones. In the next step, resulting ingots were cold-rolled to the final thickness of about 40 μ m. Then the foils were annealed in the vacuum furnace at 1270 K for 2 h and slowly cooled to the room temperature during 6 h. The base pressure during the annealing process was lower than 10⁻⁴ Pa. Thanks to that procedure, obtained samples should be homogeneous and defect-free [10]. Finally, the annealed alloys were exposed to air at 870 K for different periods of time. Each step of samples processing was followed by ⁵⁷Fe transmission Mössbauer spectroscopy (TMS) measurements which were performed at room temperature by means of a constant-acceleration POLON spectrometer of standard design, using a ⁵⁷Co-in-Rh source with a full width at half maximum (FWHM) of 0.24 mm/s.

*corresponding author; e-mail: ridczak@ifd.uni.wroc.pl

2.2. Data analysis

The measured TMS spectra were analysed using the thin absorber approximation, in terms of a sum of different number of single lines (singlets) and six-line patterns (sextets) corresponding to various isomer shifts IS, quadrupole splitting QS as well as hyperfine fields B at ^{57}Fe nuclei related to different chemical states of ^{57}Fe Mössbauer probes. For each sextet, the intensity lines ratio I_{16}/I_{34} was constant and equal to 3/1. The ratio I_{25}/I_{34} as well as three linewidths Γ_{16} , Γ_{25} and Γ_{34} were free parameters. Moreover, it was assumed that the QS in a cubic lattice is equal to zero.

The analysis of the spectra taken for annealed samples revealed that all prepared Fe–Ni, Fe–Ni–Cr, and Fe–Ni–Si alloys are in the single phase with bcc structure. In the case of annealed Fe–Ni alloys, the obtained Mössbauer

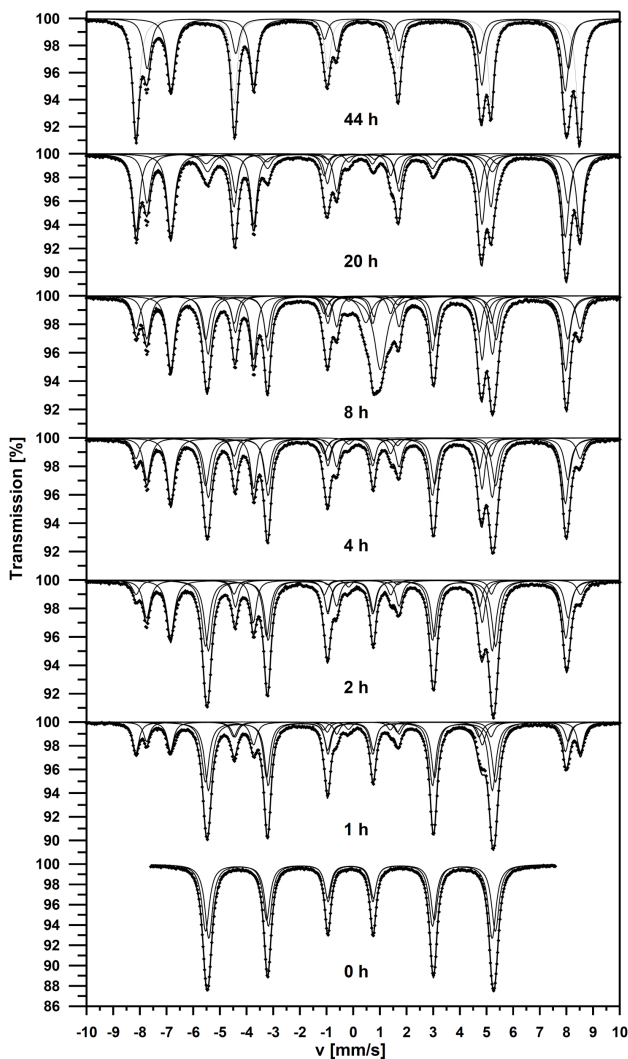


Fig. 1. The room temperature TMS spectra for the $\text{Fe}_{0.97}\text{Ni}_{0.03}$ alloys exposed to air at 870 K for the time indicated, fitted with a sum of various number of six-line patterns corresponding to different chemical state of iron atoms.

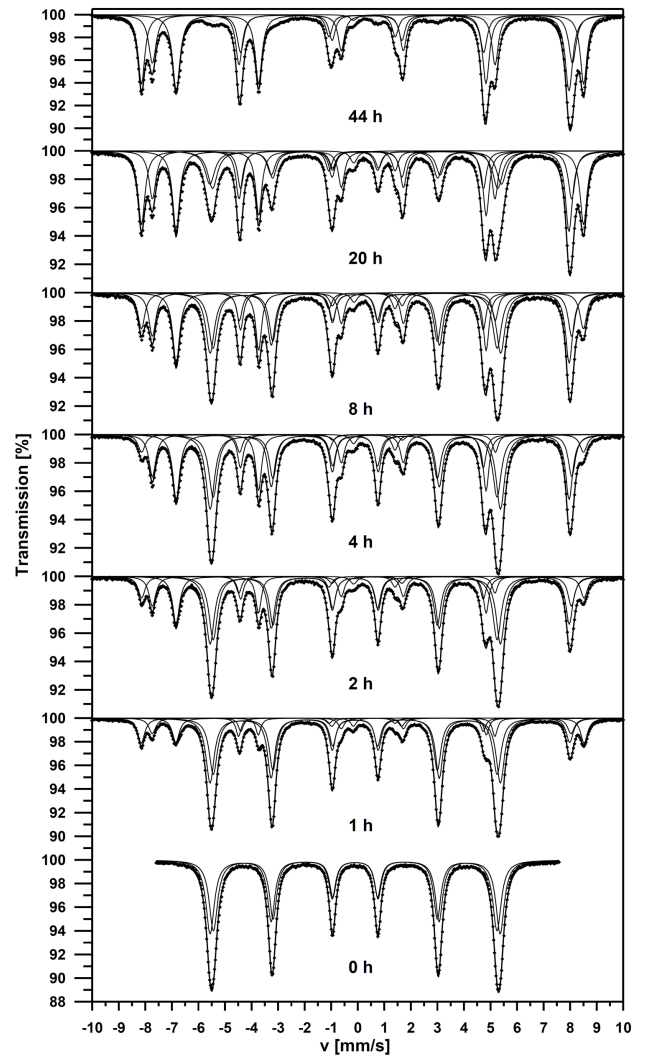


Fig. 2. As in Fig. 1, but for the $\text{Fe}_{0.95}\text{Ni}_{0.05}$ alloys.

spectra could be described by a model which assumes that the influence of n_{Ni} nickel atoms on B as well as the corresponding isomer shift IS of a subspectrum, is additive and independent of the Ni atom positions in the first two coordination shells of the nuclear probe [11]. The relationship between B , IS and n_{Ni} can be written as follows:

$$B(n_{\text{Ni}}) = B_0 + n_{\text{Ni}}\Delta B_{\text{Ni}},$$

$$\text{IS}(n_{\text{Ni}}) = \text{IS}_0 + n_{\text{Ni}}\Delta \text{IS}_{\text{Ni}}, \quad (1)$$

where ΔB_{Ni} and $\Delta \text{IS}_{\text{Ni}}$ stand for the changes of B and IS with one Ni atom in the first two coordination shells of the Mössbauer probe. To simplify the fitting procedure, the ΔB_{Ni} values were fixed. On the basis of the Mössbauer data presented in [11], it was assumed that $\Delta B_{\text{Ni}} = 0.725$ T for $\text{Fe}_{0.97}\text{Ni}_{0.03}$ and $\Delta B_{\text{Ni}} = 0.745$ T for $\text{Fe}_{0.95}\text{Ni}_{0.05}$. In the case of ternary Fe–Ni–Cr and Fe–Ni–Si alloys, this model should be extended to include the presence of n_{Cr} chromium and n_{Si} silicon atoms and their influence on B as well as IS at the ^{57}Fe nuclei. The influence of Cr atoms is also additive and independent of

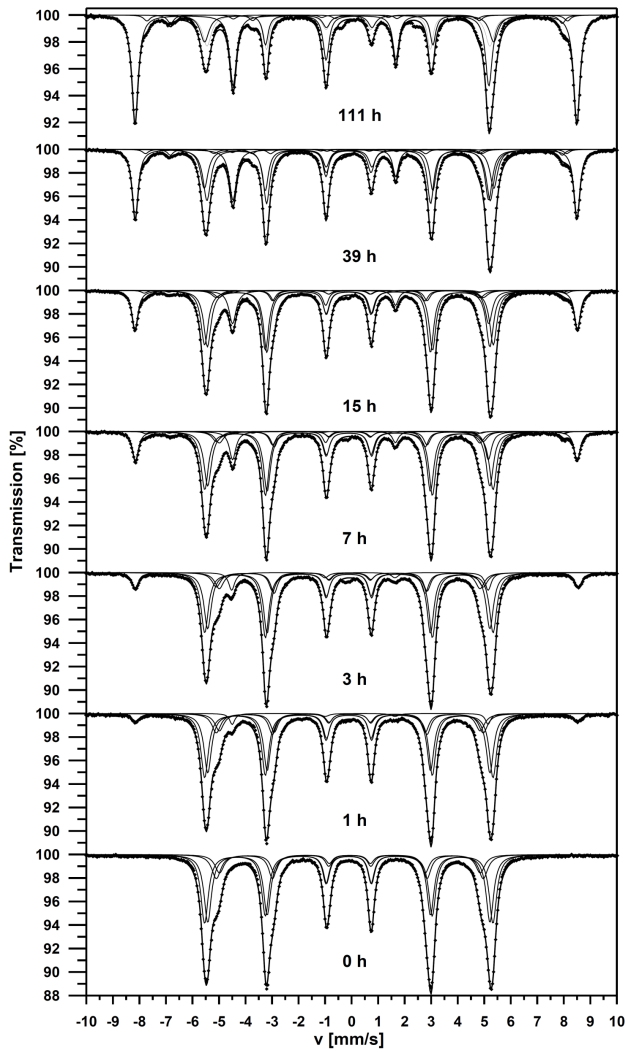


Fig. 3. As in Fig. 1, but for the $\text{Fe}_{0.94}\text{Ni}_{0.03}\text{Si}_{0.03}$ sample.

the Cr atom positions in the first two coordination shells of the nuclear probe [12], so the relationship between B , IS , n_{Ni} , and n_{Cr} for the Mössbauer spectra of annealed Fe–Ni–Cr alloys can be described by

$$B(n_{\text{Ni}}, n_{\text{Cr}}) = B_0 + n_{\text{Ni}}\Delta B_{\text{Ni}} + n_{\text{Cr}}\Delta B_{\text{Cr}},$$

$$IS(n_{\text{Ni}}, n_{\text{Cr}}) = IS_0 + n_{\text{Ni}}\Delta IS_{\text{Ni}} + n_{\text{Cr}}\Delta IS_{\text{Cr}}. \quad (2)$$

It was assumed that $\Delta B_{\text{Cr}} = -2.69$ T and $\Delta IS_{\text{Cr}} = -0.02$ mm/s [12]. In the case of Si atoms dissolved in α -Fe, the influence of silicon atoms on ^{57}Fe nuclei is different. Firstly, only silicon atoms located in the first coordination shell of the ^{57}Fe atom have an observable influence on its hyperfine parameters. Secondly, this influence cannot be described by simple additive model. In particular, the $\Delta B_{2\text{Si}}$ which is the change of B caused by the presence of two Si atoms in the first coordination shell of the Mössbauer probe is not equal to $2\Delta B_{1\text{Si}}$. $\Delta B_{1\text{Si}}$ stands for the change of B caused by the presence of one Si atom in the first coordination shell of

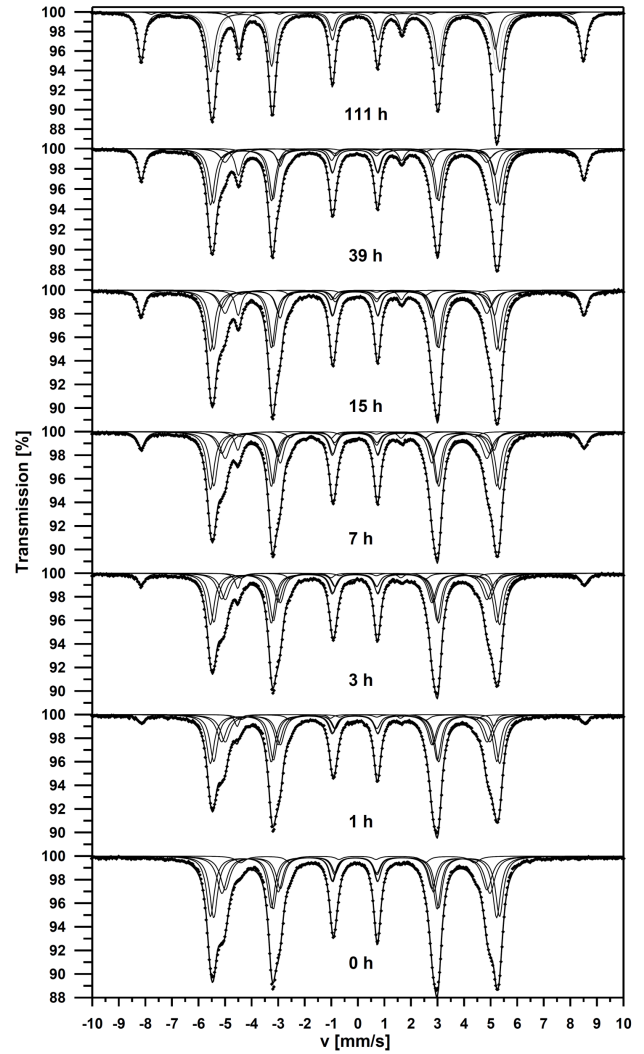


Fig. 4. As in Fig. 1, but for the $\text{Fe}_{0.92}\text{Ni}_{0.03}\text{Si}_{0.05}$ sample.

the ^{57}Fe atom. For $\text{Fe}_{0.94}\text{Ni}_{0.03}\text{Si}_{0.03}$ alloy $\Delta B_{1\text{Si}} = -2.50$ T, $\Delta B_{2\text{Si}} = -5.71$ T and for $\text{Fe}_{0.94}\text{Ni}_{0.03}\text{Si}_{0.03}$ alloy $\Delta B_{1\text{Si}} = -2.47$ T, $\Delta B_{2\text{Si}} = -5.72$ T [13].

Taking the above into account, to describe the TMS spectra measured for annealed ternary alloys with bcc structure, in the case of samples with 3 at.% of Cr or Si, four sextets were fitted. The first one corresponds to zero Ni and Cr(Si) atoms located in the neighbourhood of the ^{57}Fe . The next three are connected with the presence of 1 Ni, 1 Cr(Si) as well as both Ni and Cr(Si) atoms in vicinity of the Mössbauer probe. In the case of alloys with 5 at.% of Cr or Si, one additional sextet which correspond to 2 Cr(Si) was included.

In ^{57}Fe Mössbauer spectra of Fe–Ni, Fe–Ni–Cr and Fe–Ni–Si samples measured after exposure to air at 870 K for different periods of time, a new subspectra were observed. Three sextets and one singlet were attributed to the presence of $\alpha\text{-Fe}_2\text{O}_3$ and non-stoichiometric Fe_3O_4 as well as FeO compounds [1–3]. In particular, the mean

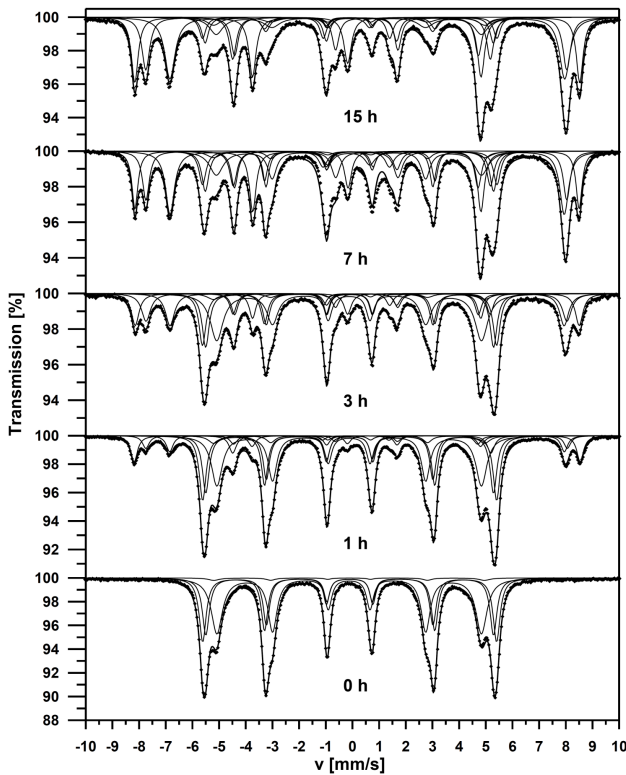


Fig. 5. As in Fig. 1, but for the $\text{Fe}_{0.94}\text{Ni}_{0.03}\text{Cr}_{0.03}$ sample.

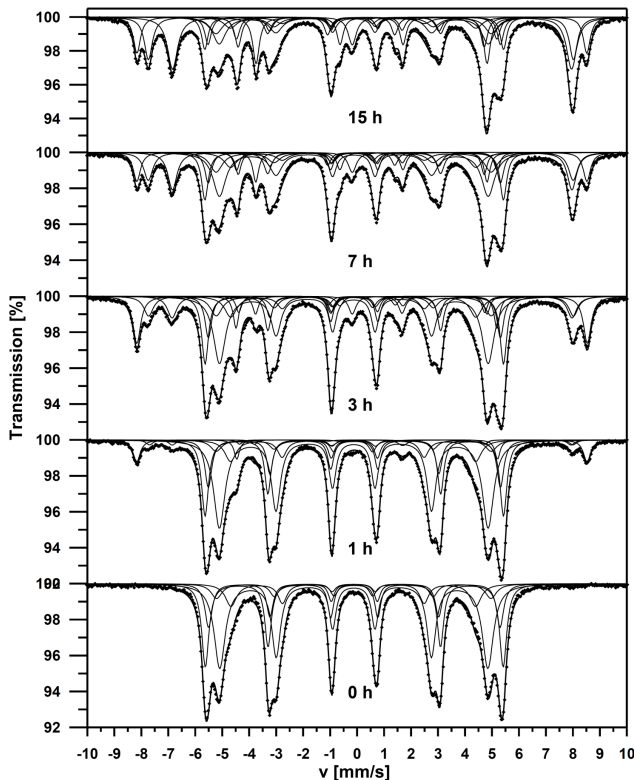


Fig. 6. As in Fig. 1, but for the $\text{Fe}_{0.94}\text{Ni}_{0.03}\text{Cr}_{0.05}$ sample.

hyperfine parameters for $\alpha\text{-Fe}_2\text{O}_3$ component were: $IS = 0.36(2)$ mm/s, $QS = -0.14(8)$ mm/s and $B = 51.6(3)$ T. The singlet with $IS = 0.59(1)$ mm/s corresponds to non-stoichiometric FeO [14] and two sextets with $IS_A = 0.24(2)$ mm/s, $QS_A < 0.1$ mm/s, $B_A = 49.1(3)$ T, and $IS_B = 0.67(3)$ mm/s, $QS_B < 0.1$ mm/s, $B_B = 45.9(4)$ T were connected with iron ions in tetrahedral (A) and octahedral (B) sites of Fe_3O_4 . Here it should be mentioned that the changes in relative intensities of these two last sextets suggest that the non-stoichiometric Fe_3O_4 were formed. Finally, the last singlet with $IS = -0.05(2)$ mm/s which appears in TMS spectra measured for Fe–Ni and Fe–Ni–Cr alloys is probably connected with paramagnetic γ' -fcc (low spin) phase [9, 15]. The measured ^{57}Fe Mössbauer spectra of Fe–Ni, Fe–Ni–Cr and Fe–Ni–Si alloys, fitted using the model described above are presented in Figs. 1–6. All the IS values presented in this paper are related to the $\alpha\text{-Fe}$ standard.

3. Results and discussion

3.1. Fe–Ni results

As the main result of the analysis, the relative intensities I of components for each spectrum were calculated. Taking into account that the relative ratio of the Lamb–Mössbauer factors $f_{\alpha\text{-Fe}} : f_{\text{FeO}} : f_{\alpha\text{-Fe}_2\text{O}_3} : f_{\text{Fe}_3\text{O}_4}$ is equal to 1 : 1 : 1.08 : 1.05 [1, 16], the fraction c_i of absorbing atoms corresponding to the I^{th} component can be calculated using I_i and f_i values using formula

$$c_i = \frac{I_i}{\sum_i \frac{I_i}{f_i}} 100\%. \quad (3)$$

The computed c_i values were used to find $c(\text{bcc})$, $c(\text{fcc})$, $c(\text{Fe}_2\text{O}_3)$, $c(\text{Fe}_3\text{O}_4)$ and $c(\text{FeO})$ parameters, which are, respectively, the fraction of absorbing ^{57}Fe atoms in bcc Fe–Ni alloy, in low spin fcc phase as well as in $\alpha\text{-Fe}_2\text{O}_3$, non-stoichiometric Fe_3O_4 and non-stoichiometric FeO compounds. As one can see, in Table I, the exposure of $\text{Fe}_{0.97}\text{Ni}_{0.03}$ and $\text{Fe}_{0.95}\text{Ni}_{0.05}$ samples to air at 870 K leads to successive and systematic growth of various iron oxides. These results are quite similar to those obtained by Channing et al. for $\text{Fe}_{0.991}\text{Ni}_{0.009}$ and $\text{Fe}_{0.90}\text{Ni}_{0.10}$ alloys [9].

In the next step, the fraction of oxidised iron atoms Fe_{OX} in $\text{Fe}_{0.97}\text{Ni}_{0.03}$ and $\text{Fe}_{0.95}\text{Ni}_{0.05}$ samples were calculated using formula

$\text{Fe}_{\text{OX}} =$

$$\frac{c(\text{Fe}_2\text{O}_3) + c(\text{Fe}_3\text{O}_4) + c(\text{FeO})}{c(\text{bcc}) + c(\text{fcc}) + c(\text{Fe}_2\text{O}_3) + c(\text{Fe}_3\text{O}_4) + c(\text{FeO})}. \quad (4)$$

In Table II, the computed Fe_{OX} values for studied Fe–Ni alloys were compared with TMS data obtained for pure iron treated in similar way [2]. As one can notice, the addition of Ni atoms slightly decreases the oxidation rate of iron atoms. This result confirms the previous observation reported by Channing et al. [9]. Finally, the analysis of the Fe_{OX} values reveals that

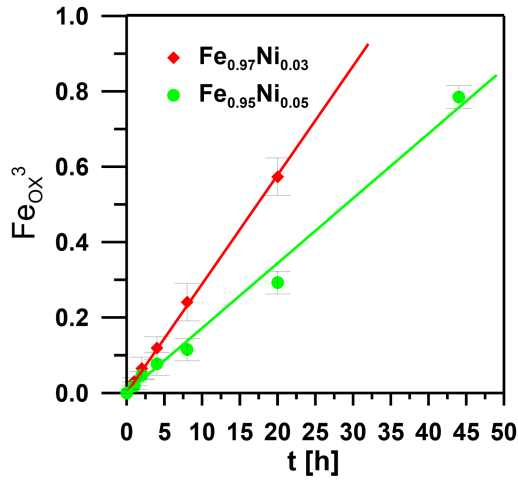


Fig. 7. The cubic oxidation kinetics of iron atoms in $\text{Fe}_{0.97}\text{Ni}_{0.03}$ and $\text{Fe}_{0.95}\text{Ni}_{0.05}$ alloys exposed to air at 870 K. The solid lines represent the best-fitting linear functions.

TABLE I

The obtained from TMS spectra fractions of absorbing ^{57}Fe atoms in bcc Fe–Ni alloy, in low spin fcc phase as well as in $\alpha\text{-Fe}_2\text{O}_3$, non-stoichiometric Fe_3O_4 , and non-stoichiometric FeO compounds. The standard uncertainties for the c parameters do not exceed 1%.

Exposure time [h]	$c(\text{bcc})$ [%]	$c(\text{fcc})$ [%]	$c(\text{Fe}_2\text{O}_3)$ [%]	$c(\text{Fe}_3\text{O}_4)$ [%]	$c(\text{FeO})$ [%]
$\text{Fe}_{0.97}\text{Ni}_{0.03}$					
0	100	0	0	0	0
1	68.0	0.8	10.6	20.6	0
2	59.2	0.6	5.4	34.8	0
4	50.2	0.6	7.9	41.3	0
8	37.4	0.4	10.0	39.1	13.1
20	16.1	0.8	27.8	55.3	0
$\text{Fe}_{0.95}\text{Ni}_{0.05}$					
0	100	0	0	0	0
1	72.6	0.8	9.9	16.7	0
2	63.2	0.7	7.6	28.5	0
4	56.6	0.8	6.1	36.5	0
8	50.5	0.8	11.1	37.6	0
20	32.5	1.1	22.2	44.2	0
44	7.1	0.7	29.2	63.0	0

TABLE II

The comparison of Fe_{OX} values obtained for $\text{Fe}_{0.97}\text{Ni}_{0.03}$ and $\text{Fe}_{0.95}\text{Ni}_{0.05}$ alloys and pure iron [1]. The standard uncertainties for the Fe_{OX} parameters do not exceed 0.02.

Exposure time [h]	Fe_{OX}		
	$\text{Fe}_{0.97}\text{Ni}_{0.03}$	$\text{Fe}_{0.95}\text{Ni}_{0.05}$	Fe [2]
0	0	0	0
1	0.31	0.27	–
2	0.40	0.36	0.84
4	0.49	0.43	0.83
8	0.62	0.49	0.87
20	0.83	0.66	1
44	–	0.92	–

for $\text{Fe}_{0.97}\text{Ni}_{0.03}$ and $\text{Fe}_{0.95}\text{Ni}_{0.05}$ alloys exposed to air at 870 K, both oxidation kinetics obey a cubic rate law

$$\text{Fe}_{\text{OX}}^3(t) = kt, \quad (5)$$

where k denotes the cubic reaction rate constant and t is an exposure time. The cubic oxidation kinetics $\text{Fe}_{\text{OX}}^3(t)$ for $\text{Fe}_{0.97}\text{Ni}_{0.03}$ and $\text{Fe}_{0.95}\text{Ni}_{0.05}$ alloys are presented in Fig. 7. The experimental data were fitted using linear regression according to Eq. (5) and the cubic reaction rate constants k at 870 K obtained for $\text{Fe}_{0.97}\text{Ni}_{0.03}$ and $\text{Fe}_{0.95}\text{Ni}_{0.05}$ samples are equal to $28.9(3) \times 10^{-3} \text{ h}^{-1}$ and $17.2(5) \times 10^{-3} \text{ h}^{-1}$, respectively.

3.2. Fe–Ni–Si results

For $\text{Fe}_{0.94}\text{Ni}_{0.03}\text{Si}_{0.03}$ and $\text{Fe}_{0.92}\text{Ni}_{0.03}\text{Si}_{0.05}$ alloys, the observed oxidation mechanism of iron atoms is quite similar (Table III). The exposure to air at 870 K results in $\alpha\text{-Fe}_2\text{O}_3$ forming first on the studied Fe–Ni–Si alloys with subsequent nucleation of non-stoichiometric Fe_3O_4 . The comparison of data presented in Tables I and III shows that addition of Si atoms to Fe–Ni alloy drastically increases the corrosion resistance. Moreover, during the thermal treatment, in both studied Fe–Ni–Si alloys, a low spin fcc phase is not formed. This result suggests that silicon atoms not only slow down the oxidation process but also stabilize bcc phase at high temperatures.

TABLE III

The obtained from TMS spectra fractions of absorbing ^{57}Fe atoms in bcc Fe–Ni–Si alloy, $\alpha\text{-Fe}_2\text{O}_3$ and non-stoichiometric Fe_3O_4 compounds. The standard uncertainties for the c parameters do not exceed 2%.

Exposure time [h]	$\text{Fe}_{0.94}\text{Ni}_{0.03}\text{Si}_{0.03}$			$\text{Fe}_{0.92}\text{Ni}_{0.03}\text{Si}_{0.05}$		
	$c(\text{bcc})$ [%]	$c(\text{Fe}_2\text{O}_3)$ [%]	$c(\text{Fe}_3\text{O}_4)$ [%]	$c(\text{bcc})$ [%]	$c(\text{Fe}_2\text{O}_3)$ [%]	$c(\text{Fe}_3\text{O}_4)$ [%]
0	100	0	0	100	0	0
1	95.6	4.4	0	96.0	4.0	0
3	92.1	7.9	0	94.5	5.5	0
7	84.4	13.6	2.0	92.7	7.3	0
15	79.3	18.5	2.2	89.7	10.3	0
39	62.1	33.0	4.9	85.3	14.7	0
111	41.1	51.8	7.1	74.9	23.3	1.8

TABLE IV

The Fe_{OX} values obtained for $\text{Fe}_{0.94}\text{Ni}_{0.03}\text{Cr}_{0.03}$ (A), $\text{Fe}_{0.92}\text{Ni}_{0.03}\text{Cr}_{0.05}$ (B), $\text{Fe}_{0.94}\text{Ni}_{0.03}\text{Si}_{0.03}$ (C), and $\text{Fe}_{0.92}\text{Ni}_{0.03}\text{Si}_{0.05}$ (D) alloys. The standard uncertainties for the Fe_{OX} parameters do not exceed 0.02.

Exposure time [h]	Fe_{OX}			
	A	B	C	D
0	0	0	0	0
1	0.04	0.04	0.19	0.09
3	0.08	0.06	0.34	0.26
7	0.16	0.07	0.54	0.33
15	0.21	0.10	0.66	0.48
39	0.38	0.15	–	–
111	0.59	0.25	–	–

The calculated fractions of oxidised iron atoms Fe_{OX} in $\text{Fe}_{0.94}\text{Ni}_{0.03}\text{Si}_{0.03}$ and $\text{Fe}_{0.92}\text{Ni}_{0.03}\text{Si}_{0.05}$ samples (Table IV) show that for these materials the oxidation kinetics obey a parabolic rate law

$$\text{Fe}_{\text{OX}}^2(t) = kt, \quad (6)$$

where k denotes the quadratic reaction rate constant and t is an exposure time. The parabolic oxidation kinetics $\text{Fe}_{\text{OX}}^2(t)$ are presented in Fig. 8 and the estimated quadratic reaction rate constants k at 870 K for $\text{Fe}_{0.94}\text{Ni}_{0.03}\text{Si}_{0.03}$ and $\text{Fe}_{0.92}\text{Ni}_{0.03}\text{Si}_{0.05}$ alloys are equal to $3.18(5) \times 10^{-3} \text{ h}^{-1}$ and $0.57(1) \times 10^{-3} \text{ h}^{-1}$, respectively. Here, it is worth noting that the quadratic reaction rate constant for $\text{Fe}_{0.97}\text{Si}_{0.03}$ alloy, treated in similar way, are lower and equal to $0.35(1) \times 10^{-3} \text{ h}^{-1}$ [2]. This fact indicates that addition of Ni atoms to Fe–Si alloys has a negative effect on the oxidation resistance.

3.3. Fe–Ni–Cr results

The exposure of $\text{Fe}_{0.94}\text{Ni}_{0.03}\text{Cr}_{0.03}$ and $\text{Fe}_{0.92}\text{Ni}_{0.03}\text{Cr}_{0.05}$ alloys to air at 870 K results in formation of two iron oxides $\alpha\text{-Fe}_2\text{O}_3$ and non-stoichiometric Fe_3O_4 as well as a low spin fcc phase (Table V). As one can notice, for this type of material, both oxides grow simultaneously and in the most measured Mössbauer spectra, the fractions of absorbing ^{57}Fe atoms in non-stoichiometric Fe_3O_4 are much larger than in $\alpha\text{-Fe}_2\text{O}_3$. That oxidation behaviour is quite similar to Fe–Cr [3]. The next important observation is connected with the systematic grow of a low spin fcc phase with exposure time. In the case of oxidised Fe–Ni samples, the calculated $c(\text{fcc})$ parameters are small (about 1%) and constant. In the case of studied

Fe–Ni–Si alloys a low spin fcc phase is not formed. This suggests that addition of Cr atoms to Fe–Ni increases a probability of bcc to fcc phase transition during exposure to air at 870 K. Finally, the obtained Fe_{OX} values (Table IV) show that for studied Fe–Ni–Cr alloys the oxidation kinetics obey a parabolic rate law described by Eq. (6) (Fig. 8). The calculated k at 870 K which are equal to $31(2) \times 10^{-3} \text{ h}^{-1}$ for $\text{Fe}_{0.94}\text{Ni}_{0.03}\text{Cr}_{0.03}$ and $15.6(6) \times 10^{-3} \text{ h}^{-1}$ for $\text{Fe}_{0.92}\text{Ni}_{0.03}\text{Cr}_{0.05}$, give clear evidence that the corrosion resistance of Fe–Ni–Cr alloys is much worse than Fe–Ni–Si.

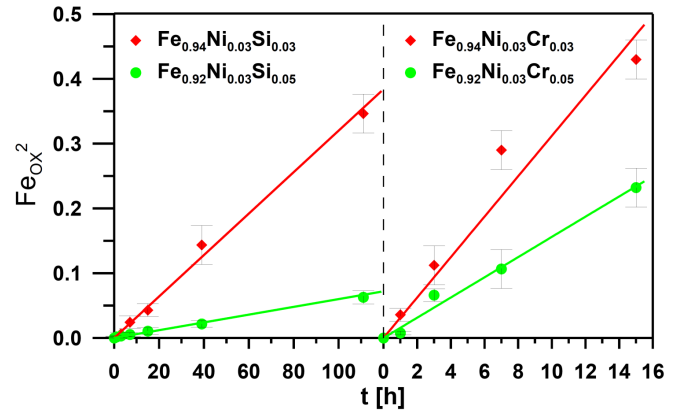


Fig. 8. The parabolic oxidation kinetics of iron atoms in $\text{Fe}_{0.94}\text{Ni}_{0.03}\text{Cr}_{0.03}$, $\text{Fe}_{0.92}\text{Ni}_{0.03}\text{Cr}_{0.05}$, $\text{Fe}_{0.94}\text{Ni}_{0.03}\text{Si}_{0.03}$, and $\text{Fe}_{0.92}\text{Ni}_{0.03}\text{Si}_{0.05}$ alloys exposed to air at 870 K. The solid lines represent the best-fitting linear functions.

The obtained from TMS spectra fractions of absorbing ^{57}Fe atoms in bcc Fe–Ni–Cr alloy, in low spin fcc phase as well as in $\alpha\text{-Fe}_2\text{O}_3$ and non-stoichiometric Fe_3O_4 compounds. The standard uncertainties for the c parameters do not exceed 2%.

TABLE V

Exposure time [h]	$\text{Fe}_{0.94}\text{Ni}_{0.03}\text{Cr}_{0.03}$				$\text{Fe}_{0.92}\text{Ni}_{0.03}\text{Cr}_{0.05}$			
	$c(\text{bcc})$ [%]	$c(\text{fcc})$ [%]	$c(\text{Fe}_2\text{O}_3)$ [%]	$c(\text{Fe}_3\text{O}_4)$ [%]	$c(\text{bcc})$ [%]	$c(\text{fcc})$ [%]	$c(\text{Fe}_2\text{O}_3)$ [%]	$c(\text{Fe}_3\text{O}_4)$ [%]
0	100	0	0	0	100	0	0	0
1	80.3	0.7	8.9	10.1	91.2	0	6.0	2.8
3	64.7	1.8	10.2	23.3	72.9	1.3	12.2	13.5
7	43.4	2.8	14.6	39.2	65.4	1.9	8.3	24.4
15	30.4	4.0	19.2	46.4	49.1	2.7	10.6	37.6

5. Conclusions

The ^{57}Fe TMS measurements allow the observation of chemical and structural changes in studied Fe–Ni, Fe–Ni–Cr and Fe–Ni–Si alloys during their exposure to air at 870 K. The results obtained for Fe–Ni samples confirm that Ni atoms dissolved in $\alpha\text{-Fe}$ have a positive effect on corrosion resistance but this effect in comparison to Cr or Si is quite small. In the case of studied Fe–Ni–Cr and Fe–Ni–Si alloys, the addition of Cr or Si atoms improve the corrosion resistance. For both ternary alloys the obtained oxidation kinetics of iron atoms could be described by parabolic oxidation law. The comparison

of the estimated quadratic reaction rate constants shows that the corrosion resistance of Fe–Ni–Cr alloys is much worse than Fe–Ni–Si. In particular, the iron oxidation rate for $\text{Fe}_{0.94}\text{Ni}_{0.03}\text{Si}_{0.03}$ is almost 10 times smaller than for $\text{Fe}_{0.94}\text{Ni}_{0.03}\text{Cr}_{0.03}$. In the case of $\text{Fe}_{0.92}\text{Ni}_{0.03}\text{Si}_{0.05}$, the oxidation rate was lower by a factor of ≈ 26 than that found for $\text{Fe}_{0.92}\text{Ni}_{0.03}\text{Cr}_{0.05}$. Moreover, in contrast to Fe–Ni and Fe–Ni–Cr alloys, in Fe–Ni–Si samples which were exposed to air at 870 K, a low spin fcc phase is not formed. Finally, taking all above into account, one can conclude that the addition of Si atoms to Fe–Ni alloy has a much more positive effect on the high-temperature atmospheric corrosion resistance than addition of Cr.

Acknowledgments

Authors would like to thank Anna Lisiecka and Aleksandra Baksalary for their assistance in samples preparation and measurements. This work was supported by the University of Wrocław under the Grant 1010/S/IFD.

References

- [1] K. Idczak, R. Idczak, R. Konieczny, *Physica B* **491**, 37 (2016).
- [2] R. Idczak, *Oxidat. Met.* **87**, 75 (2017).
- [3] R. Idczak, *Appl. Phys. A* **122**, 1009 (2016).
- [4] A. Vértes, I. Czakó-Nagy, *Electrochim. Acta* **34**, 721 (1989).
- [5] D.C. Cook, *Hyperfine Interact.* **153**, 61 (2004).
- [6] G. Chin, *IEEE Trans. Magn.* **7**, 102 (1971).
- [7] S. Jin, R.C. Sherwood, G.Y. Chin, J.H. Wernick, C.M. Bordelon, *J. Appl. Phys.* **55**, 2139 (1984).
- [8] E.F. Wassermann, P. Entel, *J. Phys. IV (France)* **05**, C8-287 (1995).
- [9] D.A. Channing, M.J. Graham, G.A. Swallow, *J. Mater. Sci.* **12**, 2475 (1977).
- [10] R. Idczak, R. Konieczny, J. Chojcan, *J. Appl. Phys.* **115**, 103513 (2014).
- [11] R. Idczak, R. Konieczny, Z. Konieczna, J. Chojcan, *Acta Phys. Pol. A* **119**, 37 (2011).
- [12] I. Vincze, I.A. Campbell, *J. Phys. F* **3**, 647 (1973).
- [13] R. Idczak, R. Konieczny, J. Chojcan, *Acta Phys. Pol. A* **129**, 367 (2016).
- [14] L.F. Checherskaya, V.P. Romanov, P.A. Tatsienko, *Phys. Status Solidi A* **19**, K177 (1973).
- [15] S. Nammas, I.A. Al-Omarib, S.H. Mahmood, *J. Alloys Comp.* **353**, 53 (2003).
- [16] D.A. Channing, M.J. Graham, *Corros. Sci.* **12**, 271 (1972).